Effect of Lipid Mixing on the Permeability and Fusion of Saturated Lecithin Membranes†

Adriana Nicolussi, Stefano Massari,* and Raffaele Colonna

ABSTRACT: The effect of phospholipid mixing on the permeability properties of multilamellar lipid vesicles (MLV) was studied. In the solid state, dimyristoylphosphatidylcholine/dipalmitoylphosphatidylcholine (DMPC/DPPC) vesicles exhibit ideal lipid miscibility; dimyristoylphosphatidylcholine/distearoylphosphatidylcholine (DMPC/DSPC) vesicles exhibit nonideal lipid miscibility at low DSPC molar fractions; dimyristoylphosphatidylcholine/dibehenoylphosphatidylcholine (DMPC/DBPC) vesicles exhibit lipid immiscibility in a large range of DBPC molar fractions. The rates of K^+, ethylene glycol, and water diffusion from these vesicles in the solid state were measured by photometric and electrometric techniques. The following results were obtained: (1) The rate of solute diffusion, which is decreased monotonically, in DMPC/DPPC MLV, by increasing the molar fractions of DPPC, exhibits maxima at 0.2 molar fraction of DSPC in DMPC/DSPC MLV and at 0.4 molar fraction of DBPC in DMPC/DBPC MLV. (2) The activation energy of the solute diffusion process abruptly decreases in approximately the same range of lipid molar fractions where nonideal lipid miscibility is present. (3) The membrane pore radius is increased by increasing the lipid nonideal miscibility. The rate of vesicle size increase, measured by absorbance changes, is decreased monotonically in DMPC/DPPC monolamellar vesicles [small unilamellar lipid vesicles (SUV)] by increasing the molar fraction of DPPC. It, however, exhibits a maximum in DMPC/DSPC SUV at 0.15 molar fraction of DSPC. A model was suggested in which the solute diffusion and the membrane fusion processes are controlled by fractures. The average width of the fractures is increased by increasing the lipid immiscibility.

As pointed out by Lee (1977), phospholipids in a crystalline solid state contain defects responsible for the formation of large-angle grain boundaries or disordered regions between two lipid domains differing in orientation or spatial arrangement. The presence of such metastable defects, in membranes whose lipids are in the solid state, appears to cause the lowering of the activation energy for translocation of solutes across the membrane and for the fusion process between lipid vesicles. Vesicles prepared by mild sonication below the lipid transition temperature, T_C, possess a permeability to lanthanide ions much higher than vesicles previously annealed above T_C (Lawaczeck et al., 1975, 1976). Extensive fusion of unannealed vesicles at temperatures near to or lower than T_C was also observed by Lawaczeck et al. (1976), who postulated that the high transport and fusion rate of unannealed structures arose from structural defects or dislocations due to discontinuous arrangement of highly ordered lipid domains. Moreover, lecithin vesicles sonicated at temperatures higher than T_C and cooled below this temperature are also unstable and are converted into larger vesicles (Suurkuusk et al., 1976; Larrabee, 1979; Schullery et al., 1980). It has been suggested that the changes occurring in the lipid packing during the passage through the phase transition may result in packing disorders that increase the contact between the hydrocarbon chains and water (Larrabee, 1979). Dark-field electron microscopy (Hui & Parsons, 1975) and electron diffraction (Hui et al., 1974) have provided direct evidence of the presence of boundaries and lipid domains, each slightly misoriented from the neighboring ones, in bilayers in the solid state. It has also been suggested that discontinuities in the membrane packing, resulting in the release of small solutes, occur in the natural membranes of *Escherichia coli* and *Bacillus subtilis* rapidly cooled below the phase transition temperature (Englesberg & Novotny, 1966; Leder & Perry, 1967; Delobbe et al., 1971; Haest et al., 1972).

These structural defects, formed under particular conditions, are occasionally present in membranes in the solid state, whereas they may be naturally created in the membrane as soon as two lipids mix nonideally. For this purpose, solid-state membranes were used in which the ideality of the lipid mixing was progressively lowered, starting from (1) ideal miscibility [dimyristoylphosphatidylcholine/dipalmitoylphosphatidylcholine (DMPC/DPPC)[1]], (2) nonideal miscibility (DMPC/DSPC), and (3) immiscibility (DMPC/DBPC). The results indicate a large increase of the vesicle fusion rate and of solute permeability in the range of lipid molar fractions where nonideal lipid miscibility is present and a corresponding abrupt decrease of the activation energy of the solute diffusion process. The lipid miscibility seems to control the solute permeability of the membranes, the solute diffusion mechanism, and the fusion process between membranes.

Materials and Methods

DMPC, DSPC, DPPC, and DBPC were purchased from Sigma. Their purity was assayed by thin-layer chromatography, and all of them were found to show a single spot. MLV were prepared as follows: a chloroform solution of phospholipids was dried in vacuo on a rotatory evaporator, and a buffer-containing solution was added above the lipid transition temperature. The flask was flushed with nitrogen, stoppered, and shaken until all lipid adhering to the bottom had been dispersed. The phospholipid suspension was slowly cooled to

† From the C.N.R. Unit for the Study of Physiology of Mitochondria, Laboratory of Biophysics and Molecular Biology, Institute of General Pathology, University of Padua, Padua, Italy. *Received August 14, 1981.*

* Address correspondence to this author at the Istituto di Patologia Generale, University of Padova, 35100 Padova, Italy.

[1] Abbreviations: P_i, inorganic phosphate; Tris, tris(hydroxymethyl)-aminomethane; DLPC, dilauroylphosphatidylcholine; DMPC, dimyristoylphosphatidylcholine; DPPC, dipalmitoylphosphatidylcholine; DSPC, distearoylphosphatidylcholine; DEPC, dieicosanoylphosphatidylcholine; DBPC, dibehenoylphosphatidylcholine; Tempo, 2,2,6,6-tetramethylpiperidinyl-1-oxy; SUV, small unilamellar lipid vesicles; MLV, multilamellar lipid vesicles.

0006-2960/82/0421-2134$01.25/0

a temperature of 15 °C (cooling rate 0.6 °C/min) and maintained at this temperature for 24 h before use. SUV were prepared as follows: lyophilized phospholipids were suspended in an aqueous solution at a concentration of approximately 1%. The suspension was maintained above the lipid phase transition temperature and ultrasonically irradiated with a Branson sonifier under a nitrogen atmosphere for 15 min. Undispersed phospholipids and titanium particles were removed by centrifugation for 20 min at 40000*g*.

The K^+ release rate was measured with a Beckman K^+ electrode connected to a Beckman pH meter and a recorder. External KCl was removed by centrifugation and resuspension of MLV in an isoosmolar solution containing choline chloride and buffer.

Absorbance changes of the lipid suspension were measured in an Eppendorf photometer at a wavelength of 334 nm or in a Perkin-Elmer Coleman 55 spectrophotometer at a wavelength of 400 nm.

Calculation of the Equivalent Pore Radius. In accordance with the treatment of Katchalsky & Curran (1967), the volume flow through a membrane, J_v, due to an osmotic pressure change, $\Delta\Pi_s$, induced by a permeant solute is

$$J_v = -L_p\sigma\Delta\Pi_s \quad (1)$$

where L_p is the filtration coefficient and σ the Staverman reflection coefficient. The latter coefficient depends on the equivalent pore radius of the membrane (Muller & Rudin, 1969). The volume flow, J_v', due to a change of osmotic pressure, $\Delta\Pi_i$, obtained with an impermeant solute is

$$J_v' = -L_p\Delta\Pi_i \quad (2)$$

where $\Delta\Pi_s = \Delta\Pi_i$, then

$$\sigma = J_v/J_v' \quad (3)$$

If the correlation between the inner vesicle volume (microliters per micromole of P_i) and the inverse value of the absorbance (micromoles of P_i per absorbance) is linear [being the slope of the straight line (*a*)], the volume flow is (Massari et al., 1972)

$$J_v = (dA/dt)(a/A_1^2)(\mu\text{mol of } P_i) \quad (4)$$

where dA is the absorbance change in the time interval dt and A_1 is the initial absorbance of the vesicle suspension. In the case of pure lecithin MLV, as demonstrated by Bangham et al. (1967), the inner liposome volume may not linearly correlate to the inverse of the absorbance. However, if the osmotic pressure change is small, and the initial rate is measured, the absorbance change is small. In this absorbance interval, the curve correlating the volume to the inverse of the absorbance can be approximated by a straight line, whose slope is *a*. Then

$$\sigma = J_v/J_v' = dA/dA' \quad (5)$$

when the initial absorbance, time interval, and amount of phospholipids are unchanged. According to this equation, the Staverman coefficient can be measured from the ratio of the absorbance changes. The theoretical family of curves (which have the pore radius as parameter) has been obtained from eq 6 of Goldstein & Solomon (1960). In the measurements of the equivalent pore radius, the osmotic pressure change was induced by 30 mM solute. The final solution was sufficiently diluted so that the errors due to the use of molarity instead of molality, variation in the refractive index, and omission of the osmotic coefficients were negligible. Moreover, low solute concentrations do not perturb the membrane structure. The molecular radii assumed by Goldstein & Solomon (1960) and Durbin (1960) for the solutes were the following: ethylene glycol, 2.25 Å; glycerol, 2.75 Å; arabinose, 3.8 Å; glucose, 4.4 Å; sucrose, 5.3 Å; raffinose, 6.2 Å.

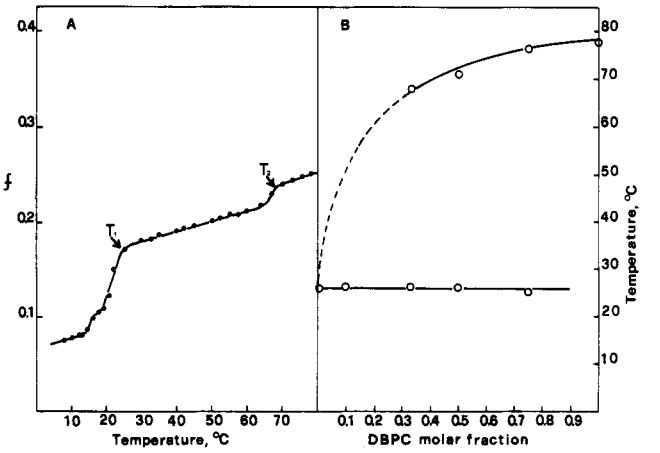

FIGURE 1: Temperature dependence of the Tempo spectral parameter. (A) The Tempo spectral parameter *f* was calculated from the amplitudes of the high-field nitroxide hyperfine signals according to the method of Shimshick & McConnell (1973). The molar fraction of DBPC in DMPC/DBPC MLV was 0.33. (B) The experimental points were obtained from the temperatures T_1 and T_2, shown in (A), where the two transitions are completed, for each lipid molar fraction.

EPR Measurements. EPR measurements were obtained with a Varian E-12 spectrometer at X band. The temperature could be controlled to within ±1 °C in the 5–90 °C range and was measured with a thermocouple in the center of the microwave cavity. The heating rate was 2 °C/10 min. The sample consisted of approximately 20 μmol of the desired mixture of lipids in a buffer solution containing 0.5×10^{-3} M Tempo.

Electron Microscopy. A drop of a suspension of 1–5 mg/mL lecithin was applied to a 300-mesh copper grid coated with collodion. After 30 s, the liquid was drawn off with a blotter, and a drop of 2% phosphotungstic acid solution (pH 7.4) was applied. After 30 s, the grid was blotted to remove excess liquid and allowed to dry. The grids were observed under a Philips 300 electron microscope operating at 60 kV.

Results

Permeability Property of the Membranes in the Solid State. Figure 1A shows a plot of a Tempo spectral parameter, *f*, calculated according to the method described by Shimshick & McConnell (1973), as a function of the temperature, for DMPC/DBPC MLV at a DBPC molar fraction of 0.33. In DMPC/DBPC MLV, the abrupt increase of the spectral parameter occurs at temperatures approximately corresponding to the calorimetrically measured solid to liquid-crystalline transition temperatures of the pure components (Ladbrooke & Chapman, 1969; Hinz & Sturtevant, 1972). The appearance of two distinct transitions in the binary mixture indicates that the two lipids behave as separate components. Figure 1B shows the phase diagram for the DMPC/DBPC system. The experimental temperatures were measured at the end of the two transition curves (T_1 and T_2, Figure 1A). The phase diagram shows that, in the solid state, the two lipids are immiscible for a large range of DBPC molar fractions.

The rate of solute diffusion across lipid membranes below the solid to liquid-crystalline phase transition temperature is very slow and can be measured only when a high solute gradient and large amounts of vesicles are used.

Figure 2 reports the rates of K^+ release from DMPC/DPPC, DMPC/DSPC, and DMPC/DBPC MLV in the solid state as a function of the lipid molar fraction; these were

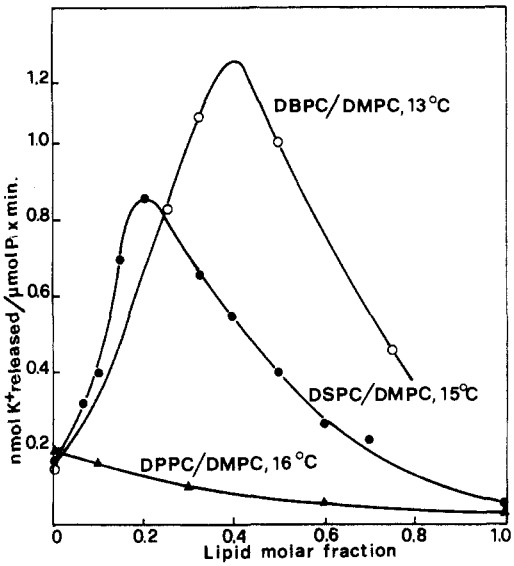

FIGURE 2: Dependence of K^+ diffusion rate on the lipid molar fractions in mixed vesicles. MLV were prepared in 0.3 M KCl and 0.01 M Tris-HCl, pH 7. A 1-μmol sample of P_i of vesicles was washed in an isoosmolar solution containing choline chloride and Tris-HCl and incubated at the temperatures shown. K^+ efflux was measured with a K^+ electrode, and the intial rates were calculated.

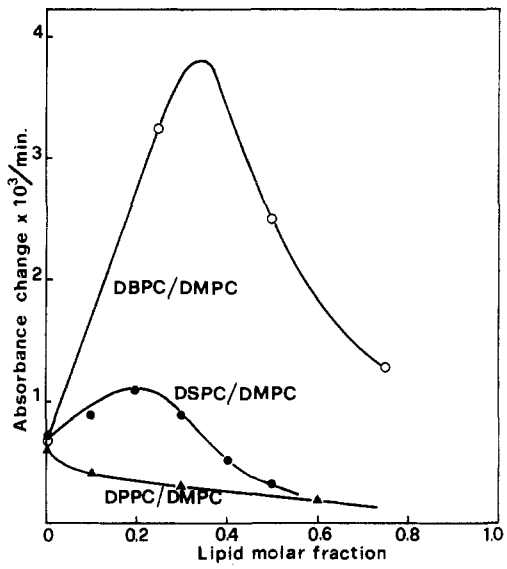

FIGURE 3: Dependence of the glycol diffusion rate on the lipid molar fractions in mixed vesicles. MLV were prepared in 0.11 M Tris-HCl, pH 7. A 1-μmol sample of P_i of vesicles was incubated, at 15 °C, in a solution containing 0.2 M ethylene glycol and 0.01 M Tris-HCl, pH 7. Absorbance changes were measured at 334 nm.

measured electrometrically. In DMPC/DPPC MLV, the rate of K^+ release is decreased monotonically by increasing the DPPC molar fractions. In DMPC/DSPC and DMPC/DBPC MLV, the rate of K^+ release exhibits a maximum at DSPC and DBPC molar fractions of 0.2 and 0.4, respectively. The rate of K^+ release at 0.4 DBPC molar fraction is higher than the rate of the 0.2 DSPC molar fraction. The lipid molar fractions where the two maxima occur do not change even at temperatures lower than those shown in Figure 2.

Figure 3 reports the photometrically measured rates of ethylene glycol uptake from DMPC/DPPC, DMPC/DSPC, and DMPC/DBPC MLV in the solid state as a function of the lipid molar fractions. The rate of the absorbance decrease is proportional to the rate of glycol uptake, provided that the vesicle volume is linearly correlated to the inverse of the absorbance and that water penetrates faster than the osmotically

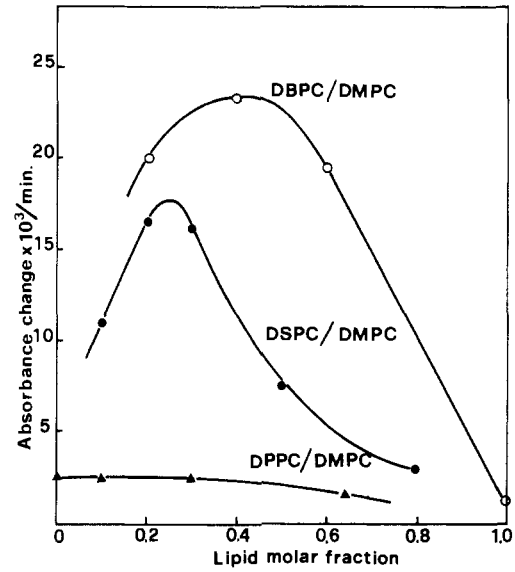

FIGURE 4: Dependence of the water diffusion rate on the lipid molar fractions in mixed vesicles. MLV were prepared in 0.02 M sucrose and 0.01 M Tris-HCl, pH 7. A 1-μmol sample of P_i of vesicles was incubated, at 14 °C, in the same medium, and the process was started after addition of 0.04 M sucrose. The absorbance changes were measured at 334 nm.

active solute (Massari et al., 1972). As pointed out earlier, the curve correlating the vesicle volume to the inverse of the absorbance can be approximated by a straight line within a short range of absorbance changes. Moreover, the activation energy of water permeation is lower than that of solute permeation through solid-state lipid bilayers, suggesting that water penetrates faster than the solute (Lawaczeck, 1979).

The dependence of the rate of glycol uptake on the lipid molar fraction shows close similarities with that of the rate of K^+ release. In fact, it decreases monotonically in DMPC/DPPC MLV by increasing the DPPC molar fraction and exhibits a maximum at 0.2 molar fraction of DSPC and at 0.4 molar fraction of DBPC in DMPC/DSPC and DMPC/DBPC MLV, respectively. Furthermore, the glycol diffusion rate at 0.4 molar fraction of DBPC is higher than the rate at 0.2 molar fraction of DSPC. Finally, the lipid molar fractions where the two maxima occur do not change even at temperatures lower than those reported in the figure. Tris-HCl may be released from MLV during the glycol uptake. However, DMPC/DBPC MLV, which are the most permeable, incubated in an isoosmolar concentration of sucrose show no absorbance change for a long period of time, indicating that the rate of Tris release is comparable to the rate of sucrose uptake. Since this rate is about 10 times lower than that of glycol uptake, we conclude that the rate of Tris-HCl release is low compared with that of glycol uptake.

Figure 4 shows the photometric measurements of the rate of water release from DMPC/DPPC, DMPC/DSPC, and DMPC/DBPC MLV in the solid state as a function of the lipid molar fraction. Sucrose, used to obtain the osmolarity jump, is impermeant to DMPC/DPPC and DMPC/DSPC MLV and slowly permeant to DMPC/DBPC MLV. Yet, the rate of water permeation in these vesicles is much higher than that of sucrose uptake. The rates of water permeation show close similarities with those of K^+ release and glycol uptake.

Activation Energy of the Diffusion Process. The general Arrhenius expression for the temperature dependency of the permeability coefficient P will be $P_0 \exp[-E_a/(RT)]$, where E_a is the activation energy. According to this equation, the logarithmic plots of the permeability against the inverse of the

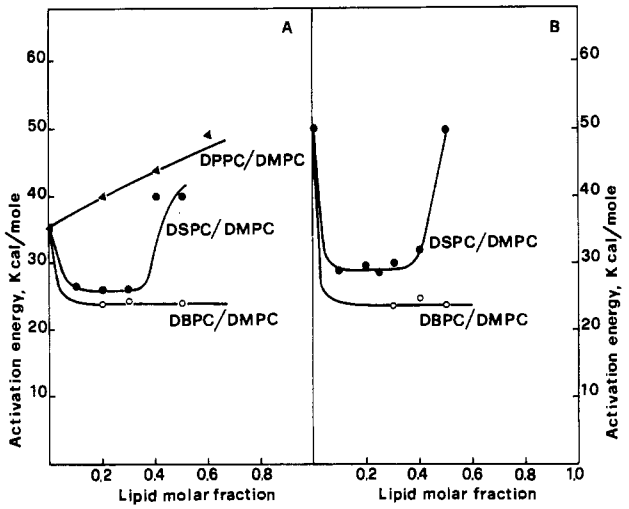

FIGURE 5: Activation energy for K^+ and glycol diffusion processes. (A) Activation energies for the glycol uptake were calculated from experiments performed as described in Figure 3. (B) The activation energies for the K^+ diffusion were calculated from experiments performed as described in Figure 2.

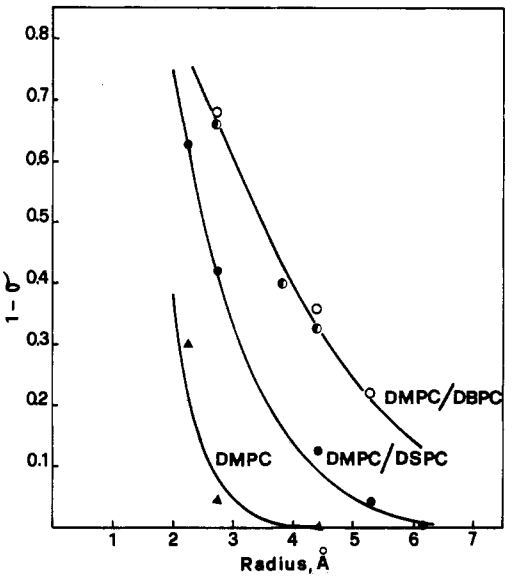

FIGURE 6: Reflection coefficient measurements. DMPC (▲), DMPC/DSPC (●), and DMPC/DBPC (○) MLV were prepared in 0.01 M Tris-HCl, pH 7, and 0.03 M permeant solute and incubated, at 14 °C, in a solution containing 0.01 M Tris-HCl, pH 7. DMPC/DBPC (◐) MLV were prepared in 0.01 M Tris-HCl, pH 7, and incubated, at 14 °C, in a solution containing 0.01 M Tris-HCl, pH 7, and 0.03 M permeant solute. The reflection coefficient σ was calculated from the absorbance change rates, due to water diffusion, as described under Materials and Methods.

absolute temperature will give straight lines with a slope of $-E_a/R$. In this study, the experimental Arrhenius plots were obtained by measuring the rate of solute diffusion instead of the permeability at the different temperatures. However, the rate of solute diffusion is proportional to the permeability coefficient since the average surface and the number of lamellae of MLV do not change. The diffusion processes studied were K^+ release, measured electrometrically, and glycol uptake, measured by absorbance changes. The temperatures used to calculate the Arrhenius plots in our experiments were restricted to the 16–19 °C range, in which a linear relationship for both diffusion processes was observed between $1/T$ and ln P. Only in the case of K^+ released from DMPC MLV does a shoulder appear in the Arrhenius plot at temperatures higher than 13 °C. This deviation from linearity takes place in the temperature interval where the lipid pretransition occurs. The pretransition in DMPC MLV occurs between 10 and 14 °C, depending on the detection technique and the experimental condition [see Lentz et al. (1978)].

Figure 5 shows the activation energies of the glycol and K^+ diffusion processes, respectively, as a function of the lipid molar fraction of mixed MLV. The activation energy of the glycol uptake increases monotonically in DMPC/DPPC MLV as the molar fraction of DPPC increases. In DMPC/DSPC and DMPC/DBPC MLV on the other hand, the activation energy decreases abruptly at the low DSPC and DBPC molar fractions and maintains its value in the whole range of lipid molar fractions where nonideal lipid miscibility is present. The same behavior is shown for the activation energy of the K^+ release. The rates of K^+ release from DMPC/DPPC MLV, and the corresponding activation energies, were difficult to measure, owing to the very low permeability of these vesicles to the electrolyte when the lipid bilayer is in the solid state.

Reflection Coefficient Measurements. The reflection coefficient, σ, was calculated from the absorbance change due to an osmotic pressure change across the membrane, according to eq 5. The osmotic change was induced by incubating MLV containing the permeant solute, in an ipoosmotic medium, rather than by adding the permeant solute externally. In fact, external addition of solutes, especially if the solutes have a high molecular weight, may induce time-dependent absorbance changes due to aggregation or fusion of vesicles or to interaction of the solute molecules with the phospholipid external layer. However, the value of σ, calculated by addition of the permeant solute outside the vesicles, does not differ appreciably from the value of σ calculated in the above described way. The data shown in Figure 6 were calculated according to eq 5, whereas the solid curves were calculated according to the method of Goldstein & Solomon (1960). The equivalent pore radii estimated from these curves were the following: 0.4 nm for DMPC MLV, 0.8 nm for DMPC/DSPC MLV containing 0.2 molar fraction of DSPC, and 1.3 nm for DMPC/DBPC MLV containing 0.4 molar fraction of DBPC. Raffinose was used as the impermeant solute throughout all the experiments. In DMPC/DPPC and DMPC/DSPC MLV, raffinose was an impermeant solute since the rate of water diffusion did not change when sucrose was used instead of raffinose in the osmotic jump experiments. However, in DMPC/DBPC MLV, raffinose induced a rate of water diffusion higher than that induced by sucrose. In the latter system, raffinose may behave as a not completely impermeant solute. The equivalent pore radius of these vesicles may therefore be a lower estimate.

Size Increase of Mixed Vesicles. The rate of size increase of SUV was measured photometrically. Figure 7 shows that DMPC/DSPC SUV exhibit a maximum in the rate of absorbance increase at a DSPC molar fraction of 0.15, whereas in DMPC/DPPC SUV, the rate of absorbance change is decreased monotonically by increasing the DPPC molar fraction. It has not been possible to form SUV from DMPC/DBPC lipid mixtures, even at low DBPC molar fractions.

In principle, through absorbance increase measurements, the formation of larger structures is detected; these structures originate either by fusion between two vesicles, by aggregation, or by a lipid diffusion process from smaller to larger vesicles. For exclusion of an aggregation mechanism, negative-stained electron micrographs of DMPC/DSPC SUV were obtained, either immediately after the sonication or after standing 24 h at 10 °C. Figure 8 shows that, at a DSPC molar fraction of 0.15, SUV are considerably enlarged after standing and that no aggregate vesicles are present.

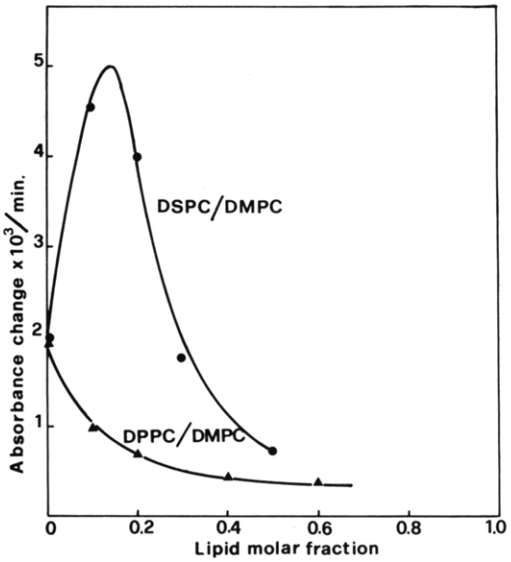

FIGURE 7: Rate of absorbance increase of a vesicle suspension. Lipid mixtures were sonified in 0.1 M Tris-HCl, pH 7. A 5 mM sample of P_i of MLV was incubated at 15 °C in the same medium, and the absorbance increase was followed at 400 nm. The rates of absorbance change were calculated by the tangents to the absorbance curve after 10-min postsonication.

Discussion

In the last decade, many experimental techniques have been used to study the phase diagrams of lecithin mixtures, including calorimetry, fluorescence, ESR, NMR, infrared spectroscopy, and dilatometry. According to many authors, when binary mixtures of phosphatidylcholines differ by two carbon atoms in the hydrocarbon chain length, such as DMPC/DPPC, there is ideal miscibility in the solid state (Shimshick & McConnell, 1973; Mabrey & Sturtevant, 1976; Lentz et al., 1976; Van Dijck et al., 1977; Luna & McConnell, 1978). When the disparity in chain length of the two phosphatidylcholines equals or exceeds six carbon atoms, such as DLPC/DSPC and DMPC/DEPC mixtures, there is immiscibility of the two components in the solid state (Mabrey & Sturtevant, 1976; Wilkinson & Nagle, 1979). As shown in Figure 1, DMPC/DBPC mixtures also exhibit immiscibility of the two lipids in the solid state within a large range of DBPC molar fractions. Much more doubts exist on the behavior of binary mixtures of phosphatidylcholines differing by four carbon atoms in chain length, such as DMPC/DSPC. Several authors have reported a horizontal solidus line in the phase diagram up to at least 0.5 DSPC molar ratio (Phillips et al., 1970; Lentz et al., 1976; Van Dijck et al., 1977), whereas others have reported a solidus line with a nonzero slope (Mabrey & Sturtevant, 1976; Gent & Ho, 1978). Shimshick & McConnell (1973) and Wilkinson & Nagle (1979) suggested that it would be rather difficult to draw conclusions about solid-state immiscibility without a sufficient precision in the shape of the solidus line of the phase diagram. Nevertheless, even if in no case there is convincing evidence for the lateral separation of a pure component, DMPC/DSPC binary mixtures behave nonideally in the solid state up to a DSPC molar fraction of 0.5–0.6.

A striking feature in solid-state membranes is the appearance of a considerable enhancement of the solute diffusion rate in the range of lipid molar fractions where lipid miscibility is nonideal. The rate of solute diffusion from MLV should depend on dimensional parameters, such as the external vesicle surface area, and the number of lipid lamellae forming the vesicles, on the solute concentration difference between outer and inner vesicle compartments, and on the membrane permeability. To correlate the rate of solute diffusion to the membrane permeability and hence to the structural properties of the membrane, it is necessary that the dimensional parameters and the solute gradient are constant when the lipid molar fraction is varied. If the solute diffusion rate in gel-state membranes would be dependent on the dimensional parameters and on the solute gradients, the rate in liquid-crystalline-state membranes should show similarly a maximum. The amount of internal lamellae in fact is the same in the two states. Moreover, the increase in the surface area and the decrease of solute gradient due to the volume expansion consequent to the lipid fluidification are independent of the molar composition of the vesicles. Finally, the permeability of liquid-crystalline membranes does not change with the lipid molar fraction since, at temperatures much higher than the transition temperature, the membrane is fully in the liquid-crystalline

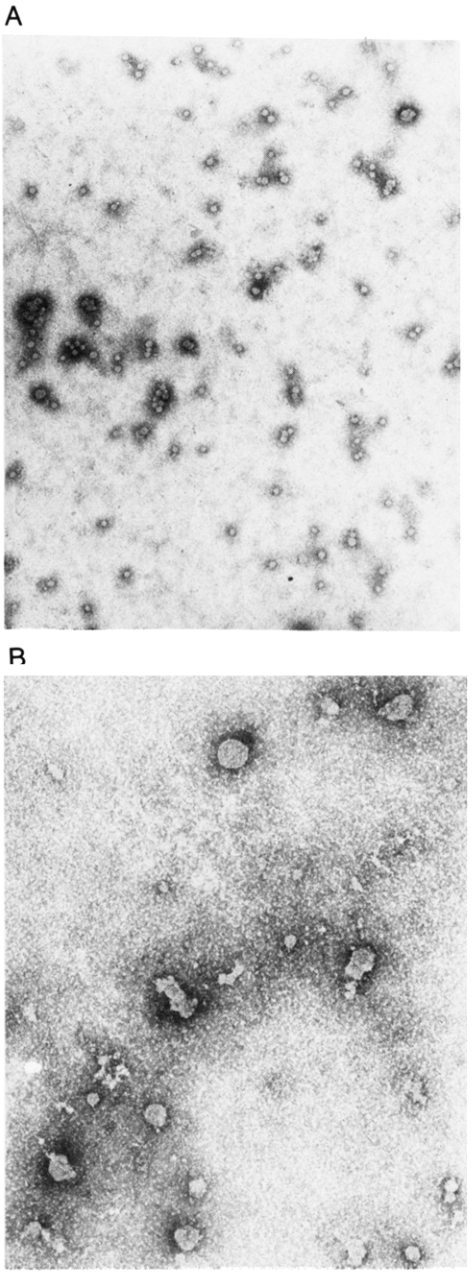

FIGURE 8: Negative-stained electron micrographs of DMPC/DSPC vesicles. (A) DMPC/DSPC SUV immediately after sonication. Magnification 39 000×. (B) The same vesicles after standing 24 h at 15 °C. Magnification 70 200×. DSPC molar ratio was 0.15.

state, the lipid miscibility is ideal, and the lipid fluidity does not change significantly in the range of lipid molar fractions where the maximum rate is found. Experiments of K^+ diffusion rate, measured at 60 °C in DMPC/DSPC MLV, show a linear decrease with DSPC molar fractions, without any maximum (not shown). Therefore, the presence of the maximum in gel-state MLV in which the lipid mixibility is nonideal should be attributed to a change of the membrane permeability. This conclusion is strengthened by the observation that the activation energy of the solute diffusion process abruptly changes in the lipid molar fraction interval where the maximum in the diffusion rate is found.

When two lipids mix nonideally, a difference in lipid–lipid interactions may originate which must lead to a preferential formation of either unlike or like lipid pairs. As a consequence, fractures may form in the bilayer, where the contact between the hydrocarbon chains and the water is increased or where the lipid mobility is increased. In both cases, the solute permeability is greatly enhanced.

The permeability coefficient of a diffusion process depends on the membrane and on permeant specific parameters which characterize the resistance to carry a molecule from the solvent into the membrane and the subsequent diffusion into the membrane. Arrhenius plots of ln P (or more exactly, ln P/T) against $1/T$ will give straight lines both when the diffusion through the water–membrane interface is rate limiting and when the diffusion through the membrane is rate limiting (Johnson & Bangham, 1969). The activation energy for ethylene glycol diffusion through lecithin MLV in the liquid-crystalline state was found to be approximately 15 kcal/mol, corresponding to the enthalpy of dehydration for this molecule (De Gier et al., 1971). On the basis of this comparison, the authors conclude that the diffusion through the hydrophobic barrier of the membrane is the rate-limiting step for nonelectrolyte diffusion. We found that the activation energy of the glycol diffusion through lecithin MLV in the solid state is higher; for DMPC, for instance, it is E_a = 35 kcal/mol. The higher activation energy presumably includes not only the enthalpy of dehydration but also the energy of diffusion into a more rigid environment. Activation energy, in fact, increases when the membrane fluidity is decreased by enhancement of the molar fraction of DPPC in DMPC/DPPC mixed vesicles, at fixed temperatures (see Figure 5). In approximately the same range of lipid molar fractions where nonideal lipid miscibility was present, the activation energy dropped to a lower constant value, 26 and 24 kcal/mol for DMPC/DSPC and DMPC/DBPC MLV, respectively. The low values of the activation energy may be explained by the formation of fractures consequent to the nonideal behavior of the lipid mixture. Glycol molecules either penetrate these partially hydrated fractures or experience a more fluid environment.

In the range of lipid molar fractions where nonideal mixing is present, the constant value of the activation energy of the glycol diffusion indicates that the mechanism of solute diffusion, hence the conformation of the fractures, does not change with the lipid composition of the vesicles. However, the permeability changes as the number of the fractures varies according to the lipid composition of the vesicles. The maximum permeability will correspond to a maximum number of these fractures in the membrane.

The activation energy for K^+ diffusion through lecithin bilayers in the liquid-crystalline state was approximately 15 kcal/mol (Papahadjopoulos & Watkins, 1967; Johnson & Bangham, 1969), and the water–membrane interface diffusion rate was suggested as the limiting step (Johnson & Bangham, 1969; Papahadjopoulos et al., 1971). The activation energy for K^+ diffusion through DMPC MLV in the solid state was about 50 kcal/mol, indicating that a different mechanism of diffusion is involved in this case. The K^+ release is similar to the glycol diffusion process in that it shows an activation energy which abruptly decreases and remains constant for approximately the same lipid molar fractions where nonideal lipid miscibility is present. The formation of fractures may again explain the smaller value of the activation energy. Maximum permeability will correspond to the maximum number of these fractures in the membrane. In this interval of nonideal lipid miscibility, the activation energy for glycol and K^+ diffusion in DMPC/DSPC MLV is slightly higher than the corresponding activation energy in DMPC/DBPC MLV. There should, therefore, be a difference between the conformation of the fractures of the two lipid mixtures. The equivalent pore radius of these membranes shows indeed that the fractures are larger in DMPC/DBPC than in DMPC/DSPC MLV. Errors made in the estimation of the equivalent pore radius are due to the assumption that the molecular radius of the anhydrous permeant solute coincides with that of the solute moving across the membranes. A solute, moving through large fractures, may indeed possess a number of hydration water molecules higher than a solute moving through narrower fractures. Consequently, the equivalent pore radii of DMPC/DSPC and DMPC/DBPC MLV would be higher than those found experimentally. Lelievre & Rich (1973) found that the reflection coefficient measured in membranes in the liquid-crystalline state showed a very poor correlation with the radius of the permeant molecule and concluded that vesicle membranes in the liquid-crystalline state are highly unlikely to contain pores. Our experiments, however, show a strong correlation between the reflection coefficient and radius of the permeant molecules in membranes in the solid state. These membranes therefore possess pore or fractures not only when the vesicles are composed of two lipids which do not mix ideally but also when the vesicles contain a pure component, such as DMPC.

The molecular mechanisms responsible for the fusion of DSPC and DPPC SUV were not studied (Suurkuusk et al., 1976; Larrabee, 1979; Schullery et al., 1980). Our findings indicate that the rate of vesicle size increase shows a maximum in DMPC/DSPC SUV approximately at the same DSPC molar fraction where a maximum of solute diffusion rate was observed in the corresponding MLV. This coincidence suggests that vesicle size increase is also a process controlled by the presence of fractures in the membrane, as suggested by Larrabee (1979).

References

Bangham, A. D., De Gier, J., & Greville, G. D. (1967) *Chem. Phys. Lipids 1*, 225.

De Gier, J., Mandersloot, J. G., Hupkes, J. V., McElhaney, R. N., & VanBeek, W. B. (1971) *Biochim. Biophys. Acta 233*, 610.

Delobbe, A., Haguenauer, R., & Rapoport, G. (1971) *Biochimie 53*, 1015.

Durbin, R. P. (1960) *J. Gen. Physiol. 44*, 315.

Englesberg, E., & Novotny, C. P. (1966) *Biochim. Biophys. Acta 117*, 217.

Gent, M. P. N., & Ho, C. (1978) *Biochemistry 17*, 3023.

Goldstein, D. A., & Solomon, A. K. (1960) *J. Gen. Physiol. 44*, 1.

Haest, C. W. M., De Gier, J., Van Es, G. A., Verkleij, A. J., & Van Deenen, L. L. M. (1972) *Biochim. Biophys. Acta 288*, 43.

Hinz, H. J., & Sturtevant, J. M. (1972) *J. Biol. Chem. 247*, 6071.
Hui, S. W., & Parsons, D. F. (1975) *Science (Washington, D.C.) 190*, 383.
Hui, S. W., Parsons, D. F., & Cowden, M. (1974) *Proc. Natl. Acad. Sci. U.S.A. 41*, 5068.
Johnson, S. M., & Bangham, A. D. (1969) *Biochim. Biophys. Acta 193*, 92.
Katchalsky, A., & Curran, P. E. (1967) *Non Equilibrium Thermodynamics in Biophysics*, Harvard University Press, Cambridge, MA.
Ladbrooke, B. D., & Chapman, D. (1969) *Chem. Phys. Lipids 3*, 304.
Larrabee, A. L. (1979) *Biochemistry 18*, 3321.
Lawaczeck, R. (1979) *J. Membr. Biol. 51*, 261.
Lawaczeck, R., Kainosho, M., Girardet, J. L., & Chan, S. I. (1975) *Nature (London) 256*, 584.
Lawaczeck, R., Kainosho, M., & Chan, S. I. (1976) *Biochim. Biophys. Acta 443*, 313.
Leder, I. G., & Perry, J. W. (1967) *Fed. Proc., Fed. Am. Soc. Exp. Biol. 26*, 394.
Lee, A. G. (1977) *Biochemistry 16*, 835.
Lelievre, J., & Rich, G. T. (1973) *Biochim. Biophys. Acta 298*, 15.
Lentz, B. R., Barenholz, Y., & Thompson, T. E. (1976) *Biochemistry 15*, 4529.
Lentz, B. R., Freire, E., & Biltonen, R. L. (1978) *Biochemistry 17*, 4475.
Luna, E. J., & McConnell, H. M. (1978) *Biochim. Biophys. Acta 509*, 462.
Mabrey, S. M., & Sturtevant, J. M. (1976) *Proc. Natl. Acad. Sci. U.S.A. 73*, 3862.
Massari, S., Frigeri, L., & Azzone, G. F. (1972) *J. Membr. Biol. 9*, 57.
Muller, P., & Rudin, D. O. (1969) *Curr. Top. Bioenerg. 3*, 157.
Papahadjopoulos, D., & Watkins, J. C. (1967) *Biochim. Biophys. Acta 135*, 639.
Papahadjopoulos, D., Nir, S., & Ohki, S. (1971) *Biochim. Biophys. Acta 266*, 561.
Phillips, M. C., Ladbrooke, B. D., & Chapman, D. (1970) *Biochim. Biophys. Acta 196*, 35.
Schullery, S. E., Schmidt, C. F., Felgner, P., Tillack, T. W., & Thompson, T. E. (1980) *Biochemistry 19*, 3919.
Shimshick, E. J., & McConnell, H. M. (1973) *Biochemistry 12*, 2351.
Suurkuusk, J., Lentz, B. R., Barenholz, Y., Biltonen, R. L., & Thompson, T. E. (1976) *Biochemistry 15*, 1393.
Van Dijck, P. W. M., Kaper, A. J., Oonk, H. A. J., & De Gier, J. (1977) *Biochim. Biophys. Acta 470*, 58.
Wilkinson, D. A., & Nagle, J. F. (1979) *Biochemistry 18*, 4244.

Glycosylation of Intracellular Sindbis Virus Glycoproteins†

John Hakimi and Paul H. Atkinson*

ABSTRACT: Oligosaccharides of purified intracellular Sindbis virus glycoproteins have been examined by high-resolution Bio-Gel chromatography. The array of glycopeptides from cellular E1 and E2 appeared similar to the glycopeptides (S1, S2, S3, and S4) found in mature virus glycoproteins described previously [Hakimi, J., & Atkinson, P. H. (1980) *Biochemistry 19*, 5619]. However, compared to its viral counterpart, intracellular E1 glycoprotein also contained larger sized mannosyl oligosaccharides. B and PE2 proteins were found to contain an array of primarily large mannosyl oligosaccharides (8–10 hexose units). No sialyl glycopeptides were found on these proteins regardless of labeling time. By contrast, the products of PE2 cleavage (E2 and E3) contained sialyl glycopeptides similar to those found in mature virus (S1, S2, and S3). E2 also contained smaller mannosyl oligosaccharides (8–5 hexose units) similar to its viral counterpart. Current evidence shows that sialyl and galactosyl transferases are in or near the Golgi region. Thus we conclude that cleavage of PE2 with a Man_8 oligosaccharide structure occurs in the Golgi region and not in the plasma membrane as suggested by others.

Sindbis virus (SbV), a membrane-maturing virus, contains a nonglycosylated nucleocapsid protein (Core) and two structural enveloped glycoproteins (E1 and E2). Chick embryo fibroblasts (CEF) infected with SbV contain six viral structural proteins and their precursors: B, PE2, E1, E2, and Core proteins and a 6000-dalton nonglycosylated polypeptide (6K) which are all translated from a single species of 26S RNA.

The precursor protein PE2 is cleaved prior to virus maturation forming E2 and E3 (or 9.8K) glycoproteins (Schlesinger & Schlesinger, 1972, 1973; Welch & Sefton, 1979). The latter is found in the culture media of SbV infected cells and is analogous to E3 glycoprotein which is associated with Semliki Forest virus (Welch & Sefton, 1979, 1980; Garoff et al., 1974, 1980; Garoff & Soderlund, 1978). The oligosaccharide structures of mature SbV glycoproteins E1 and E2 have been partially characterized (Burge & Strauss, 1970; Sefton & Keegstra, 1974; Burke, 1976; Burke & Keegstra, 1979) and have been shown to contain both sialyl (S1, S2, and S3) and a mixture of oligomannosyl (S4) glycopeptides. The viral S4 glycopeptides have been shown by the use of endoglycosidases to consist of four distinct oligomannosyl chains ranging from Man_8 to Man_5 (Hakimi & Atkinson, 1980; Hakimi et al., 1981). The intracellular glycopeptides of E1, E2, and PE2 have also been partially but not completely characterized (Sefton & Keegstra, 1974). B protein has been previously reported to be a nonstructural and nonglycosylated polypeptide containing within it both E1 and PE2 (Sefton & Burge, 1973; Schlesinger & Schlesinger, 1973). There is also evidence that B protein has a glycosylated form (Lodish, 1980; Welch & Sefton, 1979). To our knowledge no characterization of the

† From the Department of Developmental Biology and Cancer, Albert Einstein College of Medicine, Bronx, New York 10461. *Received February 26, 1981; revised manuscript received September 24, 1981.* This work was supported by National Institutes of Health Grants CA13402 and CA13330. J.H. was a Postdoctoral Fellow of the Leukemia Society of America during the course of this work. P.H.A. was an Established Investigator of the American Heart Association during the course of this work.

0006-2960/82/0421-2140$01.25/0